Dynamic Responses of Electrically Coupled Systems

NELSON G. PUBLICOVER

From the Department of Physiology, University of Nevada School of Medicine, Reno, Nevada 89557

ABSTRACT An identified pair of electrically coupled neurons in the buccal ganglion of the freshwater snail *Helisoma trivolvis* is an experimentally accessible model of electrical synaptic transmission. In this investigation, electrical synaptic transmission is characterized using (*a*) sinusoidal frequency (Bode) responses computed by Laplace transforms and (*b*) responses to brief stimuli. The frequency response of the injected neuron shows a 20-dB/decade attenuation and a phase shift from 0° at low frequencies to −90° at high frequencies. The response of a coupled cell shows a 40-dB/decade attenuation and a phase shift from 0° at low frequencies to −180° at high frequencies. A simple mathematical model of electrical synaptic transmission is described that displays each of these crucial features of the measured frequency responses. Methods are described to estimate the frequency responses of coupled systems based on presynaptic measurements. The responses of the coupled system to brief pulses of current were computed using the principle of superposition. The electrical properties of coupled systems impose a minimum delay in reaching a peak in all postsynaptic responses. The delays in the postsynaptic responses to brief stimuli are related to the electrical and anatomical parameters of coupled networks.

INTRODUCTION

The sinusoidal frequency (Bode) response is commonly used to characterize transmission lines and electrical networks (see, for example, Milhorn, 1966). In this investigation, the sinusoidal frequency response has been used to quantitatively characterize the electrophysiological responses of an electrically coupled neural system that controls secretion in a pair of acinous salivary glands. The salivary neuroeffector system of *Helisoma trivolvis* is a well-characterized, accessible model of an electrically coupled neural network (Kater et al., 1978). As in all coupled networks, electrical synapses behave as low-resistance electrical pathways that allow the exchange of ions and small molecules between adjoining cells (Bennett, 1977; Loewenstein, 1981). The functional unit of an electrical synapse is the cell-to-cell channel or connexon. The size of the pore in the connexon varies in different tissues and different species but has been estimated to be 1–3 nm in diameter by measuring dye coupling using molecules of various molecular weights (Loewenstein, 1981). Connexons are generally found in dense clusters, which appear as distinctive nodes in freeze-fracture electron micrographs and distinctive bands at the apposition of two membranes in transmission electron micrographs (Pappas and Bennett, 1966). There are a variety of terminologies

J. GEN. PHYSIOL. © The Rockefeller University Press · 0022-1295/86/04/0513/19$1.00 513
Volume 87 April 1986 513–531

and types of electrical synapses, including electrotonic junctions, gap junctions, nexus, and cell-to-cell junctions (Bennett, 1977). They are found in numerous types of excitable tissues, in a variety of organs, and across most phyla, including mammals (Sloper and Powell, 1978).

The salivary neuroeffector system of *H. trivolvis* consists of a pair of large, symmetrically located neurons (4L and 4R) that innervate the salivary glands. Each neuron can be visually identified on the dorsal surface of the buccal ganglion (Kater, 1974). 4L and 4R are electrically coupled to each other and often show nearly synchronous electrical activity under physiologic conditions. Dye coupling has been demonstrated using cobalt (Kater et al., 1978) and Lucifer yellow (Murphy et al., 1983). Cell 4 sends an axon across the buccal commissure to the contralateral cell 4. There an electrical synaptic connection is made near the soma of the contralateral neuron, and the axon continues along the esophageal trunk to innervate the contralateral acinous glands. The contralateral cell has a symmetrical arrangement. The electrical connections between cells 4L and 4R and the known morphology of the salivary neuroeffector system are illustrated schematically in Fig. 1*A*.

In this investigation, the frequency responses of this model system of electrical coupling are compared with a mathematical model of electrical synaptic transmission. Both amplitude and phase data indicate that the mathematical model is the simplest approximation that displays all of the essential features of the measured frequency responses. Experimentally, responses after the injection of steps of current are more readily accessible. Thus, the relations between the step responses and the frequency responses of the coupled network are demonstrated. The model can also be used to predict the phase lag or postsynaptic delay after brief stimuli. Postsynaptic delays are related to the mathematical, electrical, and anatomical parameters of the electrically coupled system.

METHODS

H. trivolvis is a gastropod mollusk found in freshwater lakes throughout the world (Kater, 1974). When bred in the laboratory, the snails lose their natural black pigmentation. "Red" laboratory strains were used throughout these experiments.

Snails were deshelled, and the buccal ganglion, along with structures attached to the ganglion (Kater, 1974), was dissected free of the rest of the animal. The attached structures included the salivary glands, the cerebral ganglion, and portions of the esophagus and buccal mass. Dissected snails were immersed in a solution containing (mM): 51.3 NaCl, 1.7 KCl, 4.1 $CaCl_2$, 1.5 $MgCl_2$, and 1.8 $NaHCO_3$. The physiological solution had a pH of 7.5 at room temperature.

Intracellular potentials and current injection were performed using glass micropipettes. The pipette resistance was 15–25 MΩ when the pipettes were filled with 3 M KCl. Intracellular potentials were amplified using conventional electronics (707, W-P Instruments, Inc., New Haven, CT). Current injection and data analysis were performed online using a microcomputer (System III, Cromemco Inc., Mountain View, CA).

MATHEMATICAL DERIVATIONS

Frequency Response

Models of electrically coupled networks (Bennett, 1966; Getting, 1974; Merickel et al., 1977) consist of cells represented by a membrane resistance, R_m, in parallel

with a membrane capacitance, C_m. Cells are interconnected by electrical synapses modeled by a coupling resistance, R_c. A total of N cells make up the coupled electrical load. In the present study, the membrane resistance and capacitance

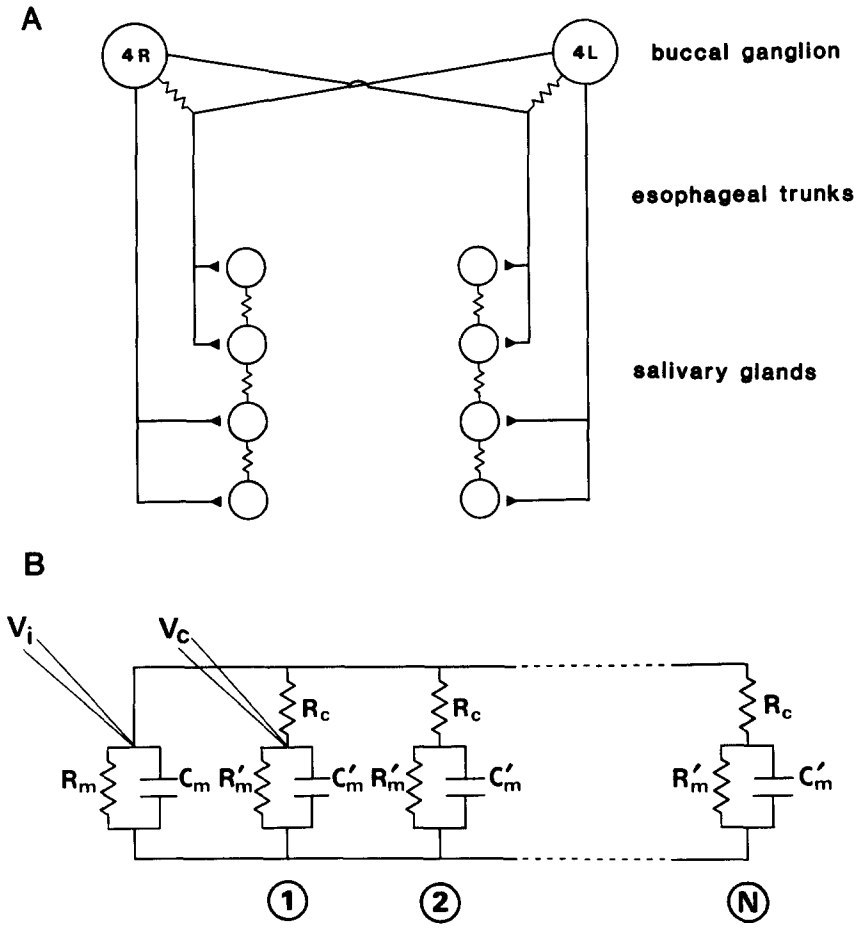

FIGURE 1. Model of the salivary neuroeffector system of *Helisoma*. (*A*) The salivary neuroeffector system consists of a pair of identified neurons, 4L and 4R, connected electrically via commissural axons. Each neuron also extends its axons to innervate both the left and right salivary glands. (*B*) Schematic representation of a model of the electrical responses of the neuroeffector system. Cell membranes consist of a parallel resistance, R_m, and capacitance, C_m. V_i represents the intracellular potential recorded from a neuron into which current is injected. N cells are coupled to the injected cell via coupling resistances, R_c. V_c represents the intracellular potential recorded from one of the coupled cells. The model can be used as a basis for the analysis of electrically coupled networks.

of the coupled load have been represented by R'_m and C'_m to distinguish them from the injected cell (Publicover, 1985). Fig. 1*B* is a schematic illustration of the model of electrical coupling. The Laplace representation of the coupled system has been derived previously (Publicover, 1985). Current was injected into

one of the cells in the coupled network. The input impedance of the injected cell, Z_i, can be expressed as

$$Z_i(s) = \frac{R'_m \cdot (1 + sT_o)}{(1 + sT_m)(1 + sT_c)}, \quad (1)$$

where the membrane time constant, T_m, is

$$T_m = R_m \cdot C_m, \quad (2)$$

the time constant of the coupled system, T_c, is

$$T_c = \left(\frac{R_c}{R_c + R'_m + N \cdot R_m}\right) T'_m, \quad (3)$$

and the system zero, T_o, is

$$T_o = \left(\frac{R_c}{R_c + R'_m}\right) T'_m. \quad (4)$$

The response of the injected cell contains a zero (T_o in the numerator) and two poles (T_m and T_c in the denominator). The log magnitude and phase of the frequency response of such a system can be expressed (Milhorn, 1966) as

$$\log_{10} A(\omega) = \log_{10}\left\{\frac{R'_m \cdot [(\omega T_o)^2 + 1]^{1/2}}{[(\omega T_m)^2 + 1]^{1/2}[(\omega T_c)^2 + 1]^{1/2}}\right\}, \quad (5)$$

$$\phi(\omega) = \tan^{-1}(\omega T_o) - \tan^{-1}(\omega T_m) - \tan^{-1}(\omega T_c), \quad (6)$$

where A is the amplitude of the response, ϕ is the phase, and ω is the angular frequency.

The transfer impedance, Z_c, seen at the site of one of the coupled cells in the system, can be expressed (Publicover, 1985) as

$$Z_c(s) = \frac{R'_m \cdot R_m}{(R_c + R'_m + N \cdot R_m) \cdot (1 + sT_m) \cdot (1 + sT_c)}, \quad (7)$$

where the membrane time constant, T_m, and the time constant of the coupled system, T_c, are as described above. The response in a coupled cell contains two poles (T_m and T_c in the denominator). The log magnitude and phase of the complex impedance (Milhorn, 1966) described by Eq. 7 are

$$\log_{10} A(\omega) = \log_{10}\left\{\frac{R_m \cdot R'_m}{(R_c + R'_m + N \cdot R_m)[(\omega T_m)^2 + 1]^{1/2}[(\omega T_c)^2 + 1]^{1/2}}\right\} \quad (8)$$

$$\phi(\omega) = -\tan^{-1}(\omega T_m) - \tan^{-1}(\omega T_c). \quad (9)$$

Eqs. 5, 6, 8, and 9 describe the frequency response of an injected cell and any of the coupled cells in an electrically coupled network.

Coupled Cell Response to a Brief Pulse

The response of a coupled cell to a pulse of current can be derived mathematically from equations computed previously (Publicover, 1985) that describe the step response. In the hyperpolarizing direction and during small deflections in the

depolarizing direction, the coupled system is approximately linear (see Fig. 3*A*), allowing the principle of superposition to be used. The principle of superposition allows a pulse to be mathematically dissociated into two transitions. A pulse can be represented as the sum of two opposing steps, separated by a pulse width, Δ. Similarly, the response to a pulse can be expressed as the sum of the responses to two opposing steps. This is illustrated in Fig. 2. Expressed mathematically:

$$V_c(t) = V_1(t) + V_2(t), \tag{10}$$

where

$$V_1(t) = -A_m \cdot \frac{T_c}{T_m} \cdot e^{-t/T_c} + A_m \cdot e^{-t/T_m} \qquad 0 < t \tag{11}$$

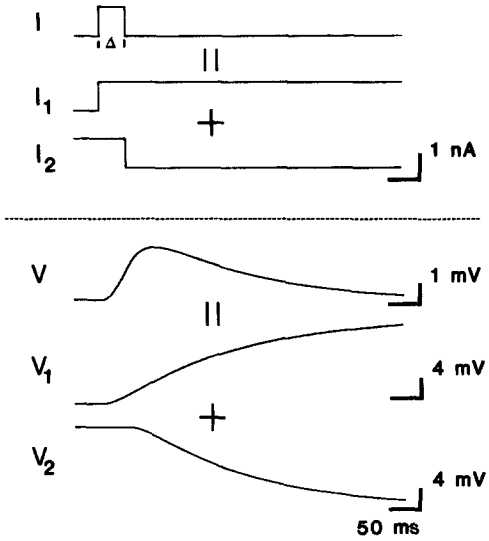

FIGURE 2. Principle of superposition used to compute the coupled response to a brief pulse. These series of simulations illustrate the principle of superposition used to calculate the response of the coupled cell to a brief pulse of current. The pulse can be expressed as the algebraic sum of a pair of steps. Similarly, the response to a pulse can be expressed as the algebraic sum of a pair of step responses.

and

$$\begin{aligned} V_2(t) &= A_m \cdot \frac{T_c}{T_m} - A_m \qquad 0 < t \leq \Delta \\ &= A_m \cdot \frac{T_c}{T_m} \cdot e^{-(t-\Delta)/T_c} - A_m \cdot e^{-(t-\Delta)/T_m} \qquad t \geq \Delta. \end{aligned} \tag{12}$$

A_m represents the amplitude of the mode in the step response associated with the membrane time constant. Expressions for A_m in terms of the electrical parameters of the model have been derived elsewhere (Publicover, 1985). The overall response to a pulse is:

$$V_C(t) = -A_m \cdot \frac{T_c}{T_m} \cdot [e^{-t/T_c} - e^{-(t-\Delta)/T_c}] + A_m \cdot [e^{-t/T_m} - e^{-(t-\Delta)/T_m}] \qquad t \geq \Delta. \tag{13}$$

The latency or delay in the response of the coupled cell is dependent on the electrical parameters of the system. The response to a very brief pulse provides an opportunity to investigate this further. Empirical studies of pulse latency (see, for example, Clapham et al., 1980) have used various points of the pulse waveform. Any identifiable point of the response can be considered using Eq. 13 as a basis. One of the easiest to measure is the peak of the coupled response to a brief pulse.

The peak latency can be identified by the point at which the derivative of the response is zero:

$$0 = \frac{dV_c(t)}{dt} = \frac{A_m}{T_c} \cdot [-e^{-t/T_c} + e^{-(t-\Delta)/T_c} - e^{-t/T_m} + e^{-(t-\Delta)/T_m}]. \tag{14}$$

After some arithmetic, the peak latency, t_{peak}, can be expressed as:

$$t_{peak} = \frac{1}{1/T_m - 1/T_c} \cdot \ln\left(\frac{1 - e^{\Delta/T_m}}{1 - e^{\Delta/T_c}}\right). \tag{15}$$

The response to an infinitesimally brief current injection or impulse response, t_{imp}, can be calculated from Eq. 15. Each of the exponential expressions can be expanded in the form of a Taylor series. The result of eliminating all terms of second order and higher is:

$$t_{imp} \equiv \lim_{\Delta \to 0} t_{peak}(\Delta) = \frac{\ln(T_c/T_m)}{1/T_m - 1/T_c}. \tag{16}$$

This is the minimum latency required for the peak of the coupled response to propagate through the system.

It is also instructive to calculate the peak latency as the pulse width becomes large, t_{long}. In this case, the exponentials in Eq. 15 dominate, so that:

$$t_{long} \equiv \lim_{\Delta \to \infty} t_{peak}(\Delta) = \frac{1}{1/T_m - 1/T_c} \cdot \ln\left(\frac{e^{\Delta/T_m}}{e^{\Delta/T_c}}\right) = \Delta. \tag{17}$$

This simply states that as the pulse becomes more like a step of current injection (Δ becomes larger), the maximum response becomes the last point at which current is applied.

Figs. 2 and 7 illustrate some applications of these equations. The amplitude of the peak response can be computed by substituting the peak latency into expressions representing the response waveform (see Fig. 2; Publicover, 1985). Other reference points (half-height, points of inflection, etc.) can be calculated in a similar fashion.

RESULTS

Sinusoidal current was injected into the salivary neuroeffector system to measure the amplitude and phase shift in both the injected and the coupled cells. Results at three different frequencies are shown in Fig. 3. At low frequencies, the responses in both the injected and the coupled cells revealed the smallest phase

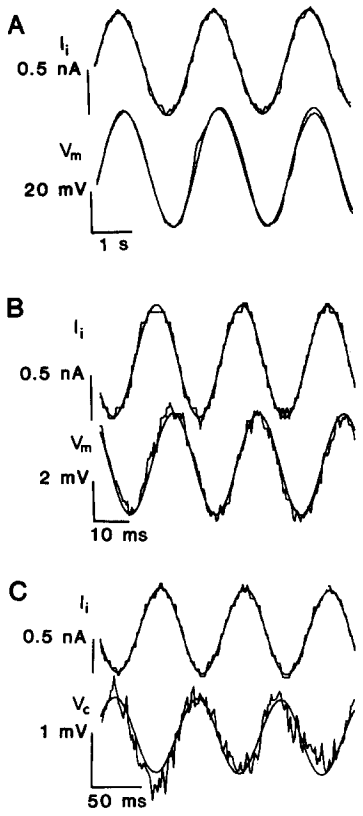

FIGURE 3. Sinusoidal responses to current injection. Current was injected into cell 4R of the buccal ganglion of *Helisoma*. In each panel, the upper trace shows the sinusoidal waveform representing the injected current. The lower traces represent the membrane potentials, recorded intracellularly. A sinusoidal function has been fit and superimposed on each trace. The parameters of the sinusoid represent the measured amplitude and phase of each response. (*A*) The low-frequency (0.42 Hz) response of the coupled system shows a large-amplitude response and a phase shift of −14°. (*B*) At high frequencies, the response in the injected cell is attenuated and approaches a phase shift of −90°. (*C*) The high-frequency response of a coupled cell is attenuated and exhibits a phase shift that approaches −180°.

shift and the largest response amplitude. Small deviations from the sinusoidal waveform occurred as a result of ongoing synaptic activity in the preparation and electronic noise in the recording apparatus. There were no instances of a phase lead at low frequencies, when the voltage response preceded the injected

current. The phase lag approached zero as the frequency of sinusoidal current injection was decreased. The amplitude of the low-frequency voltage response in the injected cell represents the steady state response determined by the input resistance of the coupled system, R'_m. The amplitude of the low-frequency response in the coupled cell represents the steady state response determined by the classical coupling coefficient (Bennett, 1966; Getting, 1974).

The low-frequency response shown in Fig. 3*A* also demonstrates the linearity of responses in the injected cell. At sufficiently low frequencies, the waveforms of responses in both injected and coupled cells matched the waveform of the input current, as long as the membrane potential did not exceed the threshold for the production of an action potential. The position of the action potential threshold varied somewhat from preparation to preparation. However, a linear dependence was consistently found between the resting membrane potential and deflections up to 20 mV in the hyperpolarizing direction. The linearity of the coupled network was also tested using steady state responses after step changes in current (Publicover, 1985) and responses to brief pulses (see Fig. 3*A*).

The amplitudes of responses at higher frequencies were expressed as a fraction of the low-frequency amplitude. Phase shifts were determined by curve-fitting the simultaneously recorded injected current and the voltage response to a sinusoidal function. The phase shift was measured as the difference in phase between the injected current and the voltage response.

As shown in Fig. 3*B*, the amplitude of the response in the injected cell was reduced at high frequencies and the phase shift lagged by almost 90° (i.e., a phase shift of −90°). The high-frequency response of the coupled cell (Fig. 3*C*) was further reduced and the voltage response was inverted compared with the injected current. In other words, the high-frequency response of the coupled cell lagged behind the injected current by 180°. The dominant source of interference during the brief intervals of current injection at high frequencies became the electronic noise of the recording apparatus because of the substantially reduced amplitude of the measured responses.

Similar measurements were repeated over a range of frequencies, resulting in Bode diagrams as shown in Figs. 4–6. The low frequencies of recordings were limited by the duration for which the neuroeffector system typically remained quiescent (i.e., did not generate an action potential). The lower-frequency range was ~0.2 Hz. The range of high frequencies was limited by the attenuation of the voltage response caused by the coupled system and the synaptic and electronic noise of the recording setup. Typically, responses could be detected up to 100 Hz in the injected cell and up to 20 Hz in the coupled cell.

The frequency (Bode) response of a typical injected cell is shown in Fig. 4. The time constants of the same preparation were also measured using the response of the presynaptic cell after a step of current (Publicover, 1985). These time constants were used to compute the relative amplitude and phase of the frequency response of the injected cell using Eqs. 5 and 6, and are shown as solid lines in both the amplitude and phase components of Fig. 4. Experimentally, the step response is much more accessible compared with sinusoidal responses over a range of frequencies. Eqs. 5 and 6 describe the relation between the parameters of the step response and the frequency response of the coupled network.

There is general agreement between the computed frequency response using the time constants of the coupled system (computed either from step responses or as a result of curve-fitting Eqs. 5 and 6) and the measured frequency response. The responses of the injected cell reveal a 20-dB/decade attenuation at high frequencies and a phase lag from 0° to −90°. No phase lags greater in magnitude than 90° were determined in any preparation (n = 5). These are essential features of the model of electrical coupling shown in Fig. 1*B*. The scatter of the data in the measured frequency response probably arises from (*a*) experimental sources and (*b*) the effects of spatially distributed load caused by the interconnecting axons. The primary source of experimental error was due to the time (~30 min) required to collect the data used to determine the frequency response.

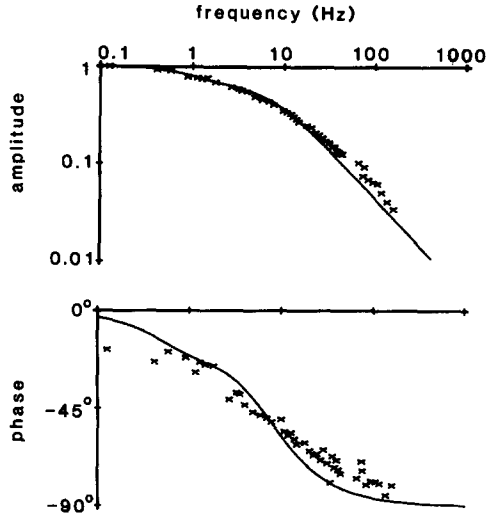

FIGURE 4. Bode response of the injected cell. Each × represents a measurement of the amplitude and phase of a sinusoidal response of the injected cell using the methods depicted in Fig. 3. The solid lines illustrate the computed frequency spectrum using parameters determined from the step response (Publicover, 1985) and Eqs. 5 and 6. The measured responses show an attenuation in amplitude of ~20 dB/decade and a phase shift from 0° at low frequencies to −90° at high frequencies. This is consistent with the impedance function representing the model of responses in the injected cell, Z_i, which contains a zero and two poles.

Physiological changes may have been occurring in preparations during this time. In other experiments in which time constants were continuously monitored for prolonged periods using current steps, variations of up to 15% were recorded over ~30-min periods. The effects of spatially distributed load or "cable-like" properties of the axons probably contribute to the phase responses and are described further in the Discussion.

The Bode response of a coupled cell is shown in Fig. 5. These data are from the same preparation as in Fig. 4. The computed frequency responses shown as solid lines in Fig. 5 are based on the time constants measured in the presynaptic cell and Eqs. 8 and 9. These data illustrate the relation between the frequency

response and the time constants determined from the step response. Furthermore, the frequency response of the coupled cell can be estimated from measurements of time constants made in the presynaptic cell.

There is general agreement between the computed frequency response using the time constants of the coupled system and the measured frequency response. The responses of the coupled cell reveal a 40-dB/decade attenuation in amplitude and a phase lag from 0° to −180°. No phase lags greater in magnitude than 180° were determined in any preparations (n = 3). These are essential features of the model of electrical coupling. The scatter of data in the measured frequency

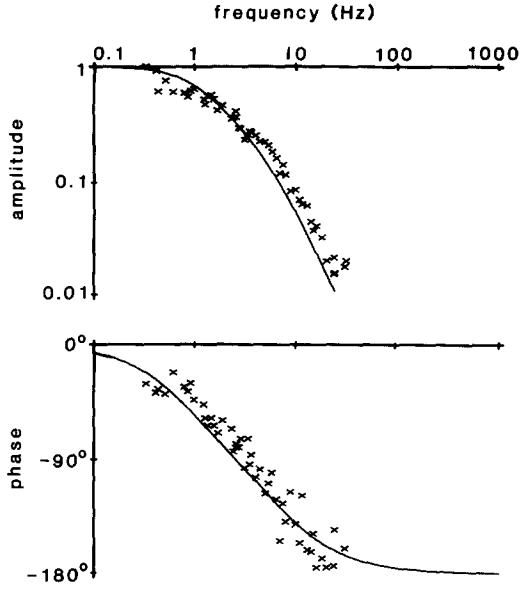

FIGURE 5. Bode response of a coupled cell. Each × represents a measurement of the amplitude and phase of a sinusoidal response of a coupled cell using the methods depicted in Fig. 3. The solid lines illustrate the computed frequency spectrum using parameters determined presynaptically from the step response (Publicover, 1985) and Eqs. 8 and 9. The measured response shows an attenuation of ~40 dB/decade and a phase shift from 0° at low frequencies to −180° at high frequencies. This is consistent with the impedance function representing the model of responses in the coupled cell, Z_c, which contains two poles.

response probably arises as a result of changes in the preparation during the data collection period and the effects of spatially distributed load caused by the interconnecting axons.

One method to manipulate the coupled network is to reduce or remove the coupled load. The effect of the coupled load can be reduced by removing junctional charge carriers (Bennett, 1977; Loewenstein, 1981), or the coupled load can be physically removed by lesion or ligation of the contralateral ganglion. The frequency response of a cell isolated by cutting away the contralateral ganglion is shown in Fig. 6. The solid lines represent the computed frequency response based on the single time constant, $T_m = R_m C_m$, of the isolated cell (Publicover, 1985) measured using the step response. The 20-dB/decade atten-

uation and the phase shift from 0° at low frequencies to −90° at high frequencies are consistent with the model of an isolated cell. The increase in the scatter of amplitude and phase measurements in the isolated cell is probably due to ongoing changes in the cell in response to the removal of its coupled host. Compared with the intact coupled network, trauma always caused an increase in the deviation between the measured and predicted frequency responses. These dynamic changes continued to occur despite allowing prolonged periods for the cell to recover after the lesion.

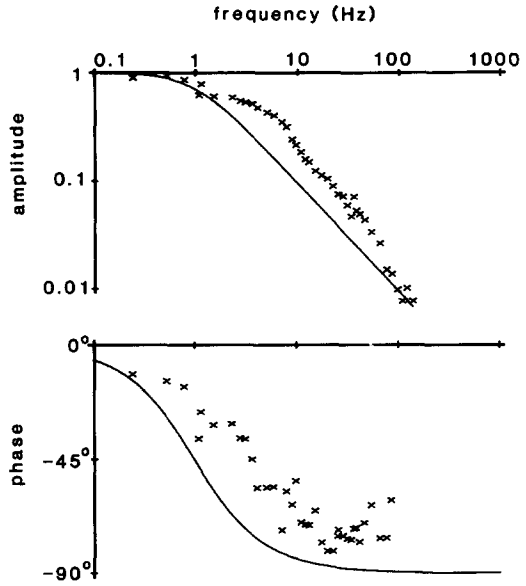

FIGURE 6. Bode response of an isolated cell. The coupled load of cell 4 was removed by lesion of the contralateral half of the buccal ganglion. The remaining ganglion was allowed to recover for 30 min. The frequency response of the isolated cell was then determined using the same methods depicted in Figs. 4 and 5. The frequency response of the lesioned cell shows an attenuation of ~20 dB/decade and a phase shift that extends from 0° at low frequencies to −90° at high frequencies. Both of these are essential features of an isolated cell represented by a single time constant, $T_m = R_m C_m$. The increase in the scatter of measurements compared with Fig. 4 and some deviation from the response predicted by the time constants of the step response probably result from the ongoing recovery of the lesioned cell during the time required to measure the frequency response.

The response of the salivary neuroeffector system to a brief depolarizing pulse is shown in Fig. 7*A*. Responses of coupled cells after brief current injections can be estimated based on presynaptic measurements (Publicover, 1985) and Eq. 13. Low-amplitude, brief hyperpolarizing and depolarizing pulses produced responses that approximated the responses of the model. Some deviation between predicted and actual responses was noted, especially early in the coupled responses. This may have been due to conductance changes in the injected cell during the delivery of current pulses or to the effects of the cable-like properties of the interconnecting axons.

The model of electrical coupling can be used as a basis to compute the responses of coupled networks to brief pulses (or "impulses"). Thus, a comparison was made to determine whether spontaneous postsynaptic potentials (PSPs) produced waveforms similar to those of the impulse response. A typical result from an

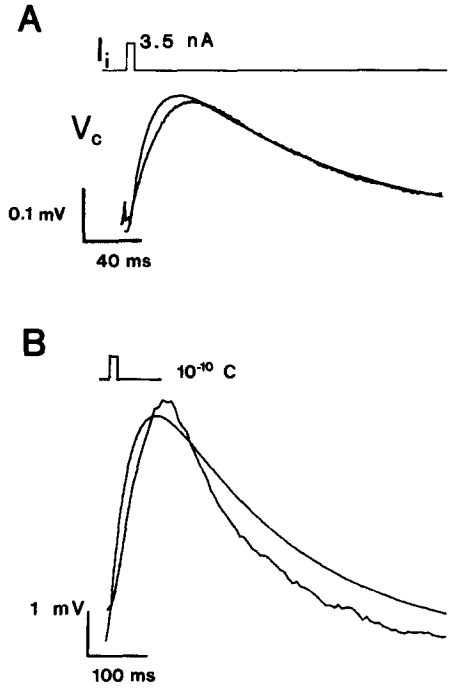

FIGURE 7. Postsynaptic potentials. (*A*) Brief depolarizing pulses, 3.5 nA in amplitude, were injected presynaptically into cell 4. The measured trace was averaged from eight postsynaptic responses. The computed trace is an estimate of the postsynaptic response based on measured responses to step changes in current in the presynaptic neuron (Publicover, 1985). Although there was some deviation from the actual postsynaptic response during the initial phase, the model provides an estimate of the coupled response to brief pulses. (*B*) This diagram shows a typical postsynaptic potential (PSP), presumably induced by one or more chemical synapses. The step response parameters of the presynaptic cell have been used to compute the impulse response of the coupled neuron. The computed response based on the model of electrical coupling is superimposed on the trace. The amplitude of the computed response has been adjusted to approximate that of the PSP and results in a charge equivalent to the injection of 10^{-10} C. The decay of the PSP is slightly faster than the computed response. This may be due to the fact that model time constants were measured presynaptically, or to prolonged conductance changes during the PSP.

excitatory PSP is shown in Fig. 7*B*. The equivalent charge (i.e., the product of the current and the injection time) necessary to produce the approximate amplitude of a typical PSP in the salivary neuroeffector system was 10^{-10} C. The waveforms of PSPs were similar to coupled impulse responses. Deviations in the

waveform may have been due to conductance changes during the PSP, the effects of spatially distributed resistances (Publicover, 1985), or the prolonged duration of conductance changes produced by a PSP.

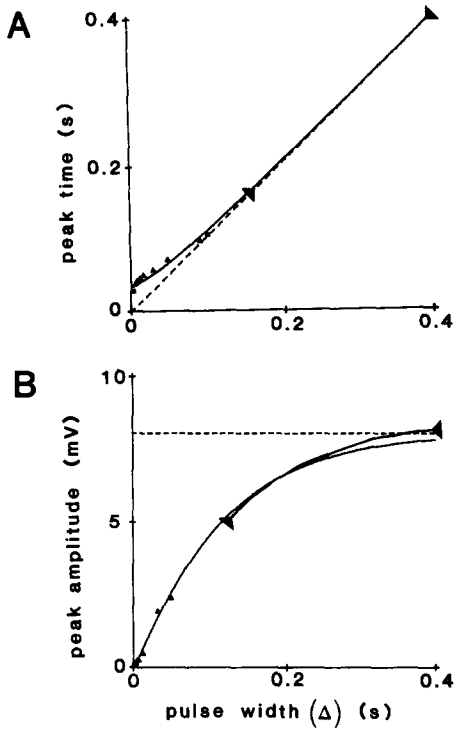

FIGURE 8. Peak of the postsynaptic response. (*A*) The time of occurrence of the peak of the postsynaptic response is plotted with respect to the duration of the presynaptic input, Δ. The small triangles represent measurements after brief current injections. Between the larger triangles, the peak of the postsynaptic response was measured at the last instant of current injection within the limitations of the recording apparatus. The dashed line represents the occurrence of the peak at the last instant of current injection (e.g., a first-order system). The solid line represents the computed position of the peak of the postsynaptic response based on the model of electrical coupling (Eq. 15). A minimum postsynaptic delay is encountered after brief presynaptic inputs. (*B*) The magnitude of the peak of the postsynaptic response is plotted with respect to the duration of the presynaptic input. The small triangles represent measurements after brief current injections. Between the larger triangles, the peak was measured as the final instant of current injection and followed the postsynaptic response to a step input. The dashed line represents the steady state postsynaptic response. The data show a linear dependence after very brief pulses and asymptote to the steady state response after inputs of longer duration.

To further investigate the responses of coupled networks to brief stimuli, responses were measured as a function of the duration of current injection. After pulses of current of varying duration, Δ, peak latency, and peak amplitude were measured. Results from one experiment are shown in Fig. 8. The minimum

delay between the application of a brief stimulus and the peak of the postsynaptic response in the salivary neuroeffector system is demonstrated in Fig. 8*A*. It was found that extremely brief pulses of current produced a finite delay in the peak response of the coupled cell. Delays after brief stimuli were much greater than the duration of the pulse. This is consistent with the model of electrical coupling. The solid line in Fig. 8*A* represents the time of the peak of the postsynaptic response computed using Eq. 15. The minimum delay in the response of a coupled network can be computed using Eq. 16.

The amplitude of the response of the coupled cell after a brief, low-amplitude current injection was proportional to both the amplitude and duration (see small triangles in Fig. 8*B*) of the input current. In other words, after brief pulses, the magnitude of the postsynaptic response is dependent upon the total charge injected. The charge is equivalent to the integral (i.e., the product, when current remains constant) of the injected current over time. As shown in Fig. 8*B*, the measured amplitudes of postsynaptic responses show a linear dependence on pulse duration after brief current pulses. As shown by the waveform between the larger triangles, the voltage response in the coupled cell after prolonged current injection reached a steady state determined by the coupling coefficient (Bennett, 1966; Getting, 1974; Publicover, 1985).

DISCUSSION

The frequency response provides a method of completely characterizing passive electrical systems. The exponential modes in step responses of injected cells have been described (Bennett, 1966; Getting, 1974; Merickel et al., 1977). More recently, postsynaptic step responses of coupled cells have also been quantitated in terms of two exponential modes (Publicover, 1985).

The essential components of the frequency response of the injected cell are: (*a*) an attenuation of 20 dB/decade as the frequency of current injection is increased, and (*b*) a phase shift that extends from 0° at low frequencies to −90° at high frequencies. Each of these features is seen in the measured Bode responses in the salivary neuroeffector system of *Helisoma*. The frequency response can also be computed from the exponential modes in the response after a step of current using Eqs. 5 and 6.

The simplest model that could describe a system with a 20-dB/decade attenuation and a phase lag from 0° to 90° is a system containing a single pole or mode, such as a simple parallel R_m-C_m circuit. However, as depicted in Fig. 5, the response of the coupled cell reveals that there are at least two modes present in the neural system. If these modes are present in the response of the injected cell, then the simplest model to describe the response consists of two poles (each contributing 20 dB/decade of attenuation and a high-frequency phase lag of 90°) and a zero (contributing 20 dB/decade of gain and a high-frequency phase lead of 90°). Eq. 1 represents such a model and is one of the simplest mathematical models of electrical coupling that display each of these components in the response of the injected cell.

The essential components of the frequency response of the coupled cell are: (*a*) an attenuation of 40 dB/decade as the frequency of current injection is

increased, and (*b*) a phase shift that extends from 0° at low frequencies to −180° at high frequencies. Each of these features is seen in the measured Bode response in the salivary neuroeffector system of *Helisoma* (Fig. 5). The postsynaptic frequency response can also be estimated from the exponential modes in responses measured presynaptically (Publicover, 1985) or postsynaptically, using Eqs. 8 and 9.

The overall features of the frequency response shown in Figs. 4 and 5 restrict the range of additional components that might be added to a compartmental model of electrical coupling. As seen from the injected cell, any additional components must contribute to the frequency response in the form of a pole-zero pair in order to maintain the observed high-frequency attenuation (20 dB/decade) and phase shift (0° to −90°). Such a pole-zero pair would be reflected in the response of the injected cell after a step change in current as an additional exponential mode. Attempts to determine a third time constant in the step response of the injected cell resulted in singular matrices using nonlinear curve-fitting techniques. This indicated that if a third time constant was present, its magnitude was insufficient to be distinct from the sources of error in the recorded signal. Within the resolution of the present techniques, the model illustrated in Fig. 1*B* is both a minimum compartmental model and a sufficient model to describe the overall responses of the coupled network.

An important issue from an experimental point of view is whether or not the frequency response of an injected cell can be used to determine the degree of electrical coupling, or whether coupling exists at all in a preparation. The 20-dB/decade attenuation and −90° phase shift are insufficient to uniquely identify a coupled network viewed from presynaptic responses. For example, an uncoupled or isolated cell produces a frequency response with a single time constant ($T_m = R_mC_m$) or pole. The frequency response of a system with a single pole consists of an attenuation of 20 dB/decade and a phase shift from 0° to −90°. Thus, the overall presynaptic frequency responses of isolated cells (see Fig. 6) are the same as those of coupled systems (see Fig. 4). However, a coupled system produces two or more exponential modes in response to a step change in current and may result in an inflection in the frequency response. Depending upon the separation of frequencies, the inflection may be subtle (as in Fig. 4) or may be quite apparent. The precise deflections in the frequency response depend upon the separation between the time constants of the coupled network. Thus, the ability to presynaptically monitor the degree of coupling depends upon the sources of noise in the recordings, the magnitude of additional modes in step responses, and the separation between time constants.

The discrete-component model illustrated in Fig. 1*B* does not account for spatially distributed loads or cable-like properties such as those contributed by long axons. Intracellular resistance, axonal resistance, and junctional resistance all impede the flow of charge from one cell into the next. Thus, in the discrete model (Fig. 1*B*), all three components probably contribute additively to the coupling resistance, R_c. In the salivary neuroeffector system of *Helisoma*, the cable-like properties of the axons (see Fig. 1*A*) have been shown to decrease the time constants of the coupled response by an average of 60% (Publicover, 1985).

It is likely that axonal resistance contributes to deviations in the frequency responses (see Figs. 4 and 5). In another coupled system, the salivary gland cells of *Helisoma*, in which closely apposed cells are electrically coupled, the reduction in the time constants of the coupled response is not apparent (Publicover, 1985). By an appropriate selection of model parameters, it is possible to compute similar responses using both the short-cable model of an axon (Rall, 1969) and the discrete model of coupling. Thus, it is likely that the two models overlap in their range of application. The model illustrated in Fig. 1*B* provides an anatomical and mathematical basis for the analysis of coupled networks. As axonal resistance and the contribution of spatially distributed loads increase, coupled systems behave more like short cables with load terminations (Rall, 1969).

The electrical characteristics of a coupled system of cells impose limitations on the ability of charge to flow from one cell to the next. This becomes most apparent when studying the impulse response of the electrically coupled system. The electrical properties of the coupled network impose a minimum peak latency upon all signals that propagate through the coupled system. The mean time constants measured in the salivary neuroeffector system (n = 52 preparations) are T_c = 27 and T_m = 180 ms (Table I). Using these mean values, the minimum

TABLE I

Mean Parameters of the Salivary Neuroeffector System (n = 52 Preparations)

Parameter	Mean	Standard deviation
T_m (ms)	180	±50
T_c (ms)	27	±8
R_m (MΩ)	150	±60
C_m (nF)	1.3	±0.6
R_c (MΩ)	56	±30
N	1.7	±0.6

peak latency in coupled responses is 60 ms (see Eq. 16). Activity only a few milliseconds in duration is seen by the coupled network as an "impulse." The waveform and peak latency of brief postsynaptic responses in *Helisoma* are minimally governed by the waveform of the presynaptic input and are largely governed by the electrical characteristics of the coupled network.

The electrical parameters of the coupled network can play a major role in the waveform of responses to brief stimuli. The mean values of electrical parameters measured (Publicover, 1985) in the salivary neuroeffector system of *Helisoma* are shown in Table I. The mathematical model of electrical coupling provides a method to predict postsynaptic responses after brief current injections, based on the anatomical and electrical parameters of the coupled system. The results of such computations are shown in Fig. 9. Typical values for the salivary neuroeffector system were used to compute the responses in Fig. 9. However, the overall relationships should apply to most coupled networks.

As described below, the differing relationships between the impulse response measurements and the electrical parameters of the coupled network (Fig. 9) provide a method to estimate the origin of physiological changes that might occur in electrically coupled networks. Alone, the four pairs of dependences

shown in Fig. 9 cannot uniquely identify which of the four electrical parameters may have changed and in which direction. However, if other evidence is available, such as changes in steady state resistance, such conclusions might be drawn. The differences can be used to investigate the effects of drugs, hormones, or other conditions that may affect the electrical responses of coupled networks.

The method takes advantage of the fact that the peak amplitude and latency

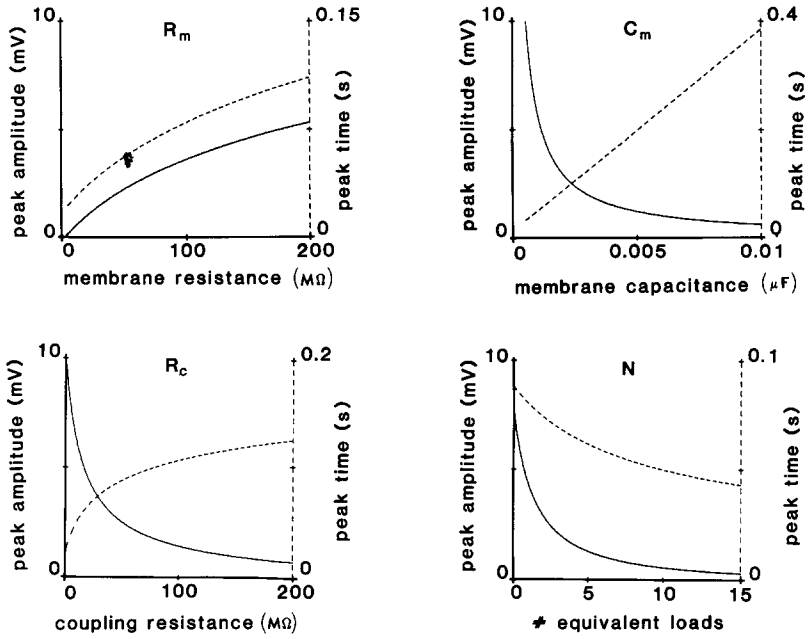

FIGURE 9. Peak latency and amplitude of the impulse response vs. the electrical parameters of the coupled system. These series of traces show the relative amplitude (solid lines) and time (dashed lines) of the peak of the coupled response based on the model of electrical coupling after a brief current injection. Both the amplitude and the latency of the peak of the coupled response increase as membrane resistance is increased. The latency increases linearly and the amplitude decreases as membrane capacitance is increased. An increase in coupling resistance also causes an increase in the latency and a decrease in the amplitude of the coupled response. An increase in the number of equivalent coupled loads decreases both the amplitude and latency of the coupled impulse response. Variations in responses to brief stimuli can be used to estimate the origin of changes in electrically coupled networks.

show a variety of different relations to the electrical parameters of the coupled system. If brief pulses of current are experimentally accessible, they can be injected into presynaptic cells. If they are not accessible, an assumption might be made that spontaneous subthreshold activity results in an impulse response and that underlying mechanisms that trigger spontaneous events remain constant throughout the duration of a series of measurements. Latency measurements can be taken from the time of current injection or (if presynaptic cells are not accessible) from the onset of the impulse response to the peak of the response.

As shown in Fig. 9, a decrease in both the latency and amplitude of the peak of the impulse response results from either a decrease in membrane resistance, R_m, or an increase in the number of coupled loads, N. Conversely, an increase in both the latency and amplitude of the peak of the impulse response results from either an increase in the membrane resistance, R_m, or a decrease in the number of coupled loads. Thus, variations of peak amplitude and duration in the same direction suggest dominant changes in membrane resistance or the coupled load.

An increase in the latency of the peak of the coupled response to an impulse and a decrease in the amplitude can result from an increase in either the membrane capacitance, C_m, or in the coupling resistance, R_c (see Fig. 9). Similarly, a decrease in the latency of the coupled response and a decrease in the amplitude can result from a decrease in either the membrane capacitance or the coupling resistance. Delays in the propagation of active events have also been studied using similar considerations (Bennett, 1966). The dependence of the peak latency on capacitance is linear, unlike the dependence of the coupling resistance. However, in experimental situations, the resolution of measurements and the range of variations in R_c may limit the ability to distinguish between a linear vs. a nonlinear dependence. On the other hand, it is unlikely that capacitance, which is generally considered to be due to the thickness and dielectric properties of the cell membrane, varies over a significant range except under specialized experimental treatments. Thus, opposing variations of the peak amplitude and duration suggest dominant changes in coupling resistance. The relationships illustrated in Fig. 9 can be used to estimate the origin of changes in electrically coupled networks.

The author wishes to thank Drs. R. W. Dykes, S. B. Kater, M. C. Mackey, and K. M. Sanders for their valuable assistance.

Some experiments were performed with support from fellowships from the Medical Research Council, Canada. This work was supported by National Institutes of Health grant AM 34406.

Original version received 17 June 1985 and accepted version received 23 December 1985.

REFERENCES

Bennett, M. V. L. 1966. Physiology of electrotonic junctions. *Annals of the New York Academy of Sciences.* 137:509–539.

Bennett, M. V. L. 1977. Electrical transmission: a functional analysis and comparison to chemical transmission. *In* Handbook of Physiology: Section I. J. M. Brookhart and V. B. Mountcastle, editors. American Physiological Society, Bethesda, MD. 357–416.

Clapham, D. E., A. Shrier, and R. L. DeHaan. 1980. Junctional resistance and action potential delay between embryonic heart cell aggregates. *Journal of General Physiology.* 75:633–653.

Getting, P. A. 1974. Modification of neuron properties by electrotonic synapses. I. Input resistance, time constant, and integration. *Journal of Neurophysiology.* 37:864–857.

Kater, S. B. 1974. Feeding in *Helisoma trivolvis*: the morphological and physiological basis of a fixed action pattern. *American Zoologist.* 14:1017–1036.

Kater, S. B., A. D. Murphy, and J. R. Rued. 1978. Control of the salivary glands of *Helisoma* by identified neurons. *Journal of Experimental Biology.* 72:91–106.

Loewenstein, W. R. 1981. Junctional intercellular communication: the cell-to-cell channel. *Physiological Reviews.* 61:829–913.

Merickel, M. B., E. D. Eyman, and S. B. Kater. 1977. Analysis of a network of electrically coupled neurons producing rhythmic activity in the snail *Helisoma trivolvis*. *IEEE Transactions on Biomedical Engineering*. 24:277–287.

Milhorn, Jr., H. T. 1966. The application of frequency analysis methods to technological and physiological systems. *In* The Application of Control Theory to Physiological Systems. W. B. Saunders Co., Philadelphia, PA. 167–193.

Murphy, A. D., R. D. Hadley, and S. B. Kater. 1983. Axotomy-induced parallel increase in electrical and dye coupling between identified neurons of *Helisoma*. *Journal of Neuroscience*. 3:1422–1429.

Pappas, G. D., and M. V. L. Bennett. 1966. Specialized junctions involved in electrical transmission between neurons. *Annals of the New York Academy of Sciences*. 137:495–508.

Publicover, N. G. 1985. Single microelectrode analysis of electrically coupled networks. *IEEE Transactions on Biomedical Engineering*. 32:491–496.

Rall, W. 1969. Time constants and electrotonic length of membrane cylinders and neurons. *Biophysical Journal*. 9:1483–1508.

Sloper, J. J., and T. P. S. Powell. 1978. Gap junctions between dendrites and somata of neurons in the primate sensori-motor cortex. *Proceedings of the Royal Society of London Series B Biological Sciences*. 203:39–47.